Cell. Mol. Life Sci. (2014) 71:2149–2164
DOI 10.1007/s00018-013-1477-z

Cellular and Molecular Life Sciences

RESEARCH ARTICLE

Combinatorial activity of *Six1-2-4* genes in cephalic neural crest cells controls craniofacial and brain development

Ricardo C. Garcez · Nicole M. Le Douarin · Sophie E. Creuzet

Received: 6 March 2013 / Revised: 16 August 2013 / Accepted: 11 September 2013 / Published online: 24 September 2013

Abstract The combinatorial expression of *Hox* genes is an evolutionarily ancient program underlying body axis patterning in all Bilateria. In the head, the neural crest (NC)––a vertebrate innovation that contributes to evolutionarily novel skeletal and neural features—develops as a structure free of *Hox*-gene expression. The activation of *Hoxa2* in the Hox-free facial NC (FNC) leads to severe craniofacial and brain defects. Here, we show that this condition unveils the requirement of three *Six* genes, *Six1*, *Six2*, and *Six4*, for brain development and morphogenesis of the maxillo-mandibular and nasofrontal skeleton. Inactivation of each of these *Six* genes in FNC generates diverse brain defects, ranging from plexus agenesis to mild or severe holoprosencephaly, and entails facial hypoplasia or truncation of the craniofacial skeleton. The triple silencing of these genes reveals their complementary role in face and brain morphogenesis. Furthermore, we show that the perturbation of the intrinsic genetic FNC program, by either *Hoxa2* expression or *Six* gene inactivation, affects Bmp signaling through the downregulation of Bmp antagonists in the FNC cells. When upregulated in the FNC, Bmp antagonists suppress the adverse skeletal and cerebral effects of *Hoxa2* expression. These results demonstrate that the combinatorial expression of *Six1*, *Six2*, and *Six4* is required for the molecular programs governing craniofacial and cerebral development. These genes are crucial for the signaling system of FNC origin, which regulates normal growth and patterning of the cephalic neuroepithelium. Our results strongly suggest that several congenital craniofacial and cerebral malformations could be attributed to *Six* genes' misregulation.

Keywords Neural crest · Hoxa2 · Signaling · Head skeleton · Holoprosencephaly · Electroporation · RNAi

Introduction

The face and the brain are phylogenetic innovations, which have evolved in the chordates phylum from the origin of vertebrate evolution. They develop from the early neurula stage by a series of concatenated events, which rely on definite morphogenetic movements, and cell migrations, proliferations, and differentiations. The precise arrangement of cell interaction and fate is coordinated by signaling pathways, where the morphogenetic action of signaling molecules are reciprocally linked to the activation of transcription factors. During evolution, the emergence of the face and brain has coincided with the specification of a pluripotent cell population in the vertebrate embryo, the neural crest (NC) [1, 2]. The NC develops from the lateral borders of the neural epithelium, and builds up the vertebrate head by providing its skeletal, dermal, and connective tissues [3, 4]. In humans, the association of craniofacial and neural defects in some congenital malformations points to the

Electronic supplementary material The online version of this article (doi:10.1007/s00018-013-1477-z) contains supplementary material, which is available to authorized users.

R. C. Garcez · S. E. Creuzet (✉)
Institut de Neurobiologie, Laboratoire Neurobiologie et Développement, CNRS-UPR3294, avenue de la Terrasse, 91198 Gif-sur-Yvette, France
e-mail: sophie.creuzet@inaf.cnrs-gif.fr

Present Address:
R. C. Garcez
Centro de Ciências Biológicas, Universidade Federal de Santa Catarina, Florianópolis, SC 88040-900, Brazil

N. M. Le Douarin
Académie des Sciences, 23, quai Conti, 75006 Paris, France

importance of reciprocal interactions between the cephalic NC and the anterior cephalic neuroepithelium. However, the molecular basis of the joint malformations of the face and the brain is still poorly understood.

Recent embryological studies have provided further evidence for the importance of the NC in cephalic ontogeny. The removal of the cephalic NC before its cells begin to migrate in the avian embryo results in the absence of a craniofacial skeleton and severe malformations of the preotic brain [5, 6], including anencephaly and absence of the telencephalon. The absence of the most rostral part of the NC, which is destined to yield the facial skeleton [also referred as the facial NC (FNC); Fig. 1a; Fig. S1], results in lower levels of Fgf8 production in both secondary brain organizers—the anterior neural ridge (ANR) and the isthmus—known to play a critical role in fore- and midbrain neurogenesis [7–9]. Moreover, the treatment of embryos from which the FNC has been removed with exogenous Fgf8 has been shown to rescue the phenotype of the concerned embryos [5, 6]. We have then shown that, at critical stages of neurogenesis, the cephalic NC is responsible for the regulation of Fgf8 production through the secretion of Bmp antagonists that counteract signals produced by the prechordal plate, the neural epithelium, and the superficial ectoderm [10]. Fgf8 production is itself regulated by Bmps [10, 11].

We have also demonstrated that the effects of NC ablation can be mimicked by the overexpression of either *Hoxa*2 alone or a combination of *Hoxa3* and *Hoxb4* in FNC cells, which do not normally express *Hox* genes. No facial structures develop when these genes are overexpressed. Moreover, the cephalic vesicles collapse and eventually degenerate, resulting in a severe, anencephalic condition [12]. These observations indicate that the molecular mechanisms governing craniofacial development differ from those controlling the ontogeny of the posterior hindbrain and trunk, in which *Hox* genes are active. It has been previously shown that, in the pharyngeal region, where a combinatorial expression of *Hox* gene regulates morphogenesis, *Hoxa2* interferes with a transcription factor of the *Six* family: Hoxa2 directly targets the expression of *Six2* and represses its activity in the NC-derived mesenchyme populating the hyoid arch [13]. This raises questions about how *Hoxa2* interferes with the morphogenetic program required for skeletogenesis in the Hox-free domain of the head.

We have investigated the mechanisms involved in these processes, by triggering the ectopic expression of *Hoxa2* in the FNC. We used the chick embryo as a model, which offers the unique advantage of allowing a precisely controlled time-, space-, and tissue-specific transgenesis. We show here that the forced expression of *Hoxa2* in FNC cells, while suppressing their skeletogenic potential, decreases the expression of genes of the *Six* family (*Six1*, *Six2*, and *Six4*) in a variable manner. The *Six1*, *Six2*, and *Six4* had similar patterns of activity in premigratory and migrating FNC cells, but their selective silencing had diverse effects, resulting in an overall reduction or partial truncation of the facial skeleton. Under these conditions, dramatic perturbations of cerebral development were observed ranging from the loss of choroid plexus and mild septal defects to alobar holoprosencephaly. By contrast, the simultaneous silencing of all three genes reproduces the adverse effects of *Hoxa2* expression, indicating that they cooperate in the control of head skeletogenesis and brain morphogenesis.

We also show that one major effect of *Hoxa2* expression or *Six* gene silencing is an upregulation of Bmp signaling in the head. Under these conditions, the overexpression of a Bmp antagonist in the FNC circumvents the deleterious effects of *Hoxa2* expression, thus rescuing face and brain development.

Fig. 1 *Hoxa2* expression in the FNC alters gene expression in the developing head. **a** Experimental design for FNC transfection and implantation into a stage-matched naive embryo at 5ss. **a′** Bilateral electroporation of NC at cephalic level with Fluorescein Dextran in a 5ss-embryo. The FNC, which extends from the mide-diencephalon down to r2, is delineated with *dotted line*; once transfected, the FNC is subjected for transplantation into a naive untransfected embryo. **a″** At 7ss, fluorescent FNC cells that have been engrafted have started to migrate (**b**–**e**) Head morphology 24 h after eletroporation and surgery. **b**, **c** External appearance and **d**, **e** internal morphology of cephalic vesicles (*dotted lines*) in control (**b**, **d**) and *Hoxa2*-transfected (**c**, **e**) embryos, showing that *Hoxa2* expression in the FNC alters face and brain development. **f**, **g** HNK1-Mab labeling of migrating FNC cells; despite morphological changes, the forced expression of *Hoxa2* in the FNC does not alter FNC cell migration. **h**–**y** Analysis of the expression of *Fgf8* (**h**–**j**), *Bmp4* (**k**–**m**), *Shh* (**n**–**p**), *Wnt8b* (**q**–**s**, *arrowheads*; *dotted lines* indicate the boundary between the diencephalon posteriorly and the telencephalon anteriorly), *Noggin* (**t**–**v**) and *Six2* (**w**–**y**) in control (**h**, **k**, **n**, **q**, **t**, **w**), *Hoxa2*-transfected (**i**, **l**, **o**, **r**, **u**, **x**), and *Six2*-silenced (**j**, **m**, **p**, **s**, **v**, **y**) embryos. While *Six2* expression is inhibited in the FNC-derived mesenchyme, its expression in the pharyngeal endoderm persists after *Hoxa2* activation or *Six2* silencing in FNC cells. Changes in gene expression are shown with *arrowheads* (**z**) RT-PCR analysis of *Hoxa2*, *Noggin*, *Dan*, and *Six2* expression in NF-derived cells grown in vitro for 24 h, taken from r4 to r8 NC, FNC, and *Hoxa2*-transfected and *Six2*-silenced FNC. *Di* diencephalon, *Mes* mesencephalon, *Rh* rhombencephalon, *Tel* telencephalon

Materials and methods

Microsurgery

Experiments were carried out on chick embryos at the 5- to 6-somite stage (5–6 ss, i.e. 30 h of incubation at 38 °C). Chick embryos were prepared for *in ovo* surgery as previously described [14]. The fate map of the cephalic neural primordium [15] was used as a reference for determining

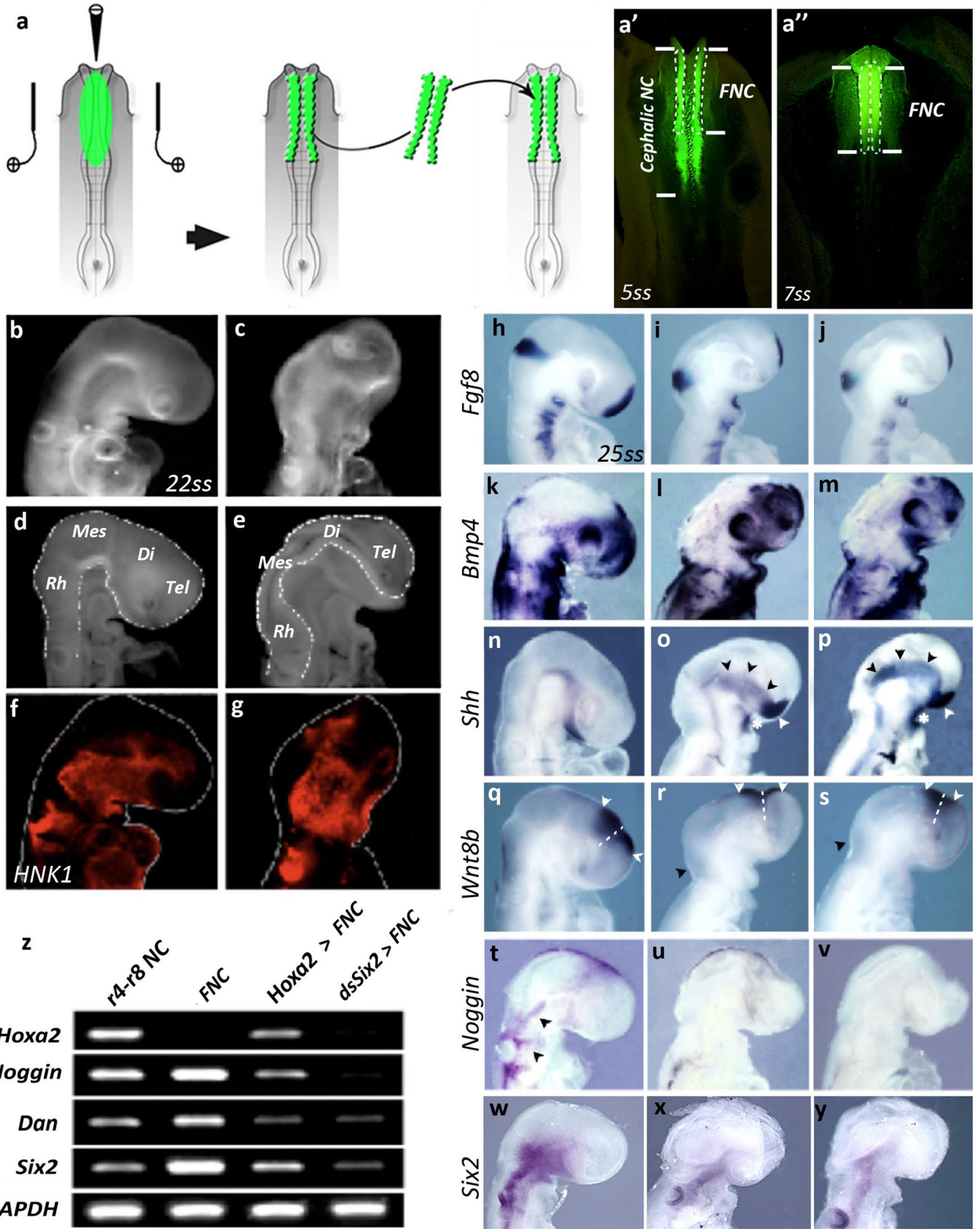

the presumptive level of the encephalic structures extending from the mid-diencephalon down to r8. According to these fate maps, the surgical and molecular manipulations were performed on the FNC, which extends from the mid-diencephalon down to rhombomere2 (r2) included (Fig. 1a).

Double-stranded RNA synthesis and electrophoration with exogenous nucleic acid

dsRNA were synthesized from cDNAs encoding the targeted genes [16]. In contrast to studies carried out in mammals, in which dsRNA yield unspecific blockade of protein synthesis, no such effects were ever detected in chicken embryos. ([17] and references therein). dsRNA-driven gene silencing results in highly specific gene inactivation.

According to these procedures, dsRNA molecules were synthesized from the cDNA encoding *Six1*, *Six2*, and *Six4*. For control series, solutions of non-annealed sense plus anti-sense RNA strands corresponding to the sequences of the targeted genes were used at the same concentration for *in ovo* electroporation, according to the same paradigm. In parallel, we also did some control experiments using dsRNA designed against *Hoxa2* for electroporation of FNC cells. As these cells are normally devoid of *Hoxa2* expression, the outcome of these experiments was similar to the control series, thus confirming the specificity of the dsRNA-driven gene silencing strategy.

Depending on the experimental series, the dsRNA molecules were used at different concentrations: functional assays on brain development were yielded with solutions of 600 ng/µl dsRNA but resulted in a high proportion of dead embryos beyond E5. The shortcoming of these series precluded the analysis of the consequences of *Six* gene silencing on craniofacial development. So, for examination of E8 skeletogenic development, silencing experiments were carried out with solutions of 300 ng/µl dsRNA. Gain-of-function experiments involving *Hoxa2* retroviral construct [12] and *Six2* gene expression vector [18] were performed with solutions of 1 µg/µl of constructs. Replication competent retroviral constructs used in this study are designed to allow for the overexpression of the insert but not produce viral particles. The ectopic activity of the gene of interest is therefore restricted to the transfected cells (i.e. FNC cells) and their progenies.

In ovo electroporations were performed in 5–6ss chick embryos. Briefly, exogenous nucleic acids in 0.01 % Fast Green (Sigma) were injected into the cephalic neural groove. Together with exogenous nucleic acid sequences, Fluorescein Dextran was coelectroporated in order to visualize and track the FNC-derived cells. Bilateral electroporation was achieved by placing two anodes on the vitelline membrane flanking the head of the embryo and one cathode against the anterior region of the embryo [12] The dsRNA molecules, retroviral or plasmidic constructs were delivered to the FNC cells by a series of five 27-V pulses (T830 BTX; Genetronics, San Diego, CA, USA). The bilaterally transfected chick neural folds, extending from the diencephalon down to r2, were then surgically excised and homotopically implanted into a stage-matched untransfected host.

Embryo processing

For whole-mount preparations, the control and experimental embryos were harvested in sterile PBS then fixed in 4 % formaldehyde. After extensive washes in PBS, embryos were dehydrated in graduate methanol and permeabilized by cold-shock in 100 % methanol at −20 °C for 45 min. After rehydratation in PBS, embryos were subjected to hybridization for gene expression analysis or immunocytochemsitry. Embryos subjected to histological analysis were fixed in 60 % ethanol, 10 % formaldehyde, 10 % acetic acid, dehydrated, and embedded in paraffin. Six-µm-thick sections were collected on Superfost-Plus slides, and processed for either hybridization or immunocytochemistry.

Whole-mount LTR staining and immunocytochemistry

In control and experimental series, NC cell migration and cell proliferation were visualized by whole-mount immunocytochemistry with monoclonal antibodies (Mab) against HNK1 (CD57; Santa Cruz Biotechnology) and phosphorylated histone3 (PhH3; Sigma), respectively, in E2.5 embryos [12]. Cell death was detected by whole-mount Lysotracker Red (LTR; Invitrogen) staining, as previously described [19]. Quantification of cell proliferation and death was then performed on vibratome sections.

Cartilage staining

Chondrogenic structures from E8 embryos were visualized after fixation in 80 % ethanol, 20 % acetic acid, and 0.015 % Alcian Blue 8GX for 16 h, extensive washing in 100 % ethanol, and clearing in 1 % KOH and 20 % glycerol.

In situ hybridization

Whole-mount in situ hybridization [20] was performed with the probes for *Fgf8* [21], *Shh* [22], *Bmp4* [23], *Noggin* [24], and *Wnt8b* [25] transcripts. When necessary, double hybridizations with FITC-tagged riboprobes were performed by tyramide signal amplification (Perkin-Elmer). *Six* gene riboprobes were generated with the following specific primer pairs for cDNA amplification by PCR and cloning with the pCR®-TOPO system (Invitrogen): *Six1* (For.5′- CGAACCC CGGATCCCATTGCG -3′;Rev.5′- GCAGCACCGCCGCG TTAAGA -3′), *Six2* (For.5′- GCGTCAATGAACGGGA ATAA -3′; Rev.5′- AGCGGTTTAAGAGCCCAGAT -3′), and *Six4* (For.5′- CCACATCCGCTCTCCAGCTCG -3′; Rev.5′- TGATGTCAGTGATGGACACCCCG -3′). GAPDH expression was used as internal reference in all PCR experiments. SyBR green assays were normalized to GAPDH activity using the following primer pair: For.5′- TCCAGGAGCGTGACC-CCAGC -3′; Rev.5′- TGCCAGGCAGTTGGTGGTGC -3′.

RNA probes were synthesized with the Riboprobe Combination System kit (Promega) and labeled with UTP-digoxygenin (Boehringer). After whole-mount hybridization, some embryos were dehydrated in ethanol, permeabilized in toluene, and embedded in paraffin for sectioning.

Microscope image acquisition

Images of whole-mount embryos were acquired on a LEICA MZ-FLIII stereomicroscope equipped with a X-Cite series 120Q, as a source of UV light, and a Qimaging cooled micropublisher camera driven by the Qcapture software.

RT-PCR analysis of gene expression in vitro

The molecular profile of the electroporated neural folds was determined by RT-PCR. The *Hoxa2*-treated, *Six2*-silenced FNC and r4–r8 NC were microdissected and cultured in vitro for 24 h in DMEM supplemented with 10 % FCS. NC cells were then harvested for cDNA preparation (SuperScript™ III; Invitrogen) and RT-PCR analysis for *Hoxa2*, *Six2*, *Noggin*, *Dan, Sox9, Runx2,* and *GAPDH*. RT-PCR primers for specific target genes were designed in Primer-BLAST tools: *Hoxa2* For.5′- TTTTTCTCCGCGGGGGCTGC -3′; Rev.5′- GGCTGGGGATGGTCTGCTCG -3′. *Noggin* For.5′- GGCTGGGGATGGTCTGCTCG -3′; Rev.5′- TATAGGACCGGGCAGAAGGT -3′; *Dan* For.5′- AGGAGAACATGCCCGCAGAG -3′; Rev.5′- ATCCTGCAGACAGCCCTTGG -3′; *Sox9* For.5′- TCTCCGTTTTCTCCTCCCCT -3′; Rev.5′ –CTTGAGGTCGGGTGTTCTCC -3′.

Quantitative RT-PCR

The isolation of RNA was performed using an RNeasy Mini Kit (Qiagen) according to the manufacturer's instructions. After isolation, RNA was treated with DNase I (Invitrogen) to digest contaminating DNA. 1 μg of RNA sample was then used for reverse transcription and synthesis of cDNA using Superscript III system (Invitrogen). Quantitative real-time PCR was performed on an AB7300 (Applied Biosystems) using SYBR Green PCR Master Mix (Applied Biosystems). The level of target gene expression was compared to GAPDH gene activity and measured by comparative Pfaffl method [26]. The statistic analysis was performed using ANOVA/Turkey tests.

Results

Hoxa2 effects on gene expression in the developing head

We investigated the molecular changes resulting from *Hoxa2* activation in FNC cells, by bilaterally electroporating these cells with an RCAS construct driving *Hoxa2* expression before they began to migrate, in chick embryos at the 5–6 somite stage (ss). *Hoxa2* activity was restricted to FNC cells, by dissecting out the transfected neural folds and transplanting them into a naive recipient chick at the same stage (Fig. 1a). In parallel, control experiments were carried out with an empty RCAS construct, according to the same procedure. Morphological differences were observed between experimental embryos and controls 24 h after surgery (E2.5; $n = 8$). Transgenic embryos had much smaller heads, with a different morphology, including conspicuous atrophy of the pre-otic encephalic vesicles (Fig. 1b–e). However, NCC emigration from the FNC was similar in control and *Hoxa2*-transfected embryos: NC-derived mesenchymal cells massively colonized the 1st branchial arch (BA1) and the nasofrontal bud (Fig. 1f, g).

We hypothesized that the morphological defects in *Hoxa2*-transgenic embryos might result from the disturbance of signaling pathways, such as those involving *Fgf8*, *Bmp4*, *Shh*, and *Wnt8b*. *Fgf8* transcript levels in the ANR, BAs, and isthmus were significantly lower than normal [21] after *Hoxa2* activation in the FNC (Fig. 1h, i; $n = 5$), this situation being reminiscent of that resulting from the removal of the FNC [5, 6]. Under this condition, *Bmp4* expression has been shown to counteract Fgf8 signaling at this stage [11]. However, in *Hoxa2*-transgenic embryos, the amount of Bmp4 transcripts was unaffected in the maxillo-mandibular, retro-ocular, nasofrontal, and BA ectoderm (Fig. 1k, l; $n = 5/5$). The absence of the FNC has been shown to result in a ventralization of the encephalic neuroepithelium, as demonstrated by laterally extended *Shh* expression [6]. Ectopic *Hoxa2* activation in FNC cells resulted in a similar lateral expansion of *Shh* expression (Fig. 1n, o; arrowheads; $n = 6/6$), together a decrease in the size of the prosencephalic and mesencephalic alar plates. At that stage, the domain of *Wnt8b* expression straddles the dorsal part of the anterior diencephalon and posterior telencephalon (Fig. 1q, white arrowheads), from which the choroid plexi normally develop in the lateral and third ventricles (Fig. 1q, dotted lines); [25, 27]. It is also expressed at the dorsal rhombencephalic midline. In *Hoxa2* transgenic embryos, *Wnt8b* was much less strongly expressed in the prosencephalon (Fig. 1r; white arrowheads) and not expressed at all in the rhombencephalon (Fig. 1r; black arrowhead; $n = 6$). Thus, *Hoxa2* expression in the FNC-derived mesenchyme had a deleterious effect on the dorso-ventral molecular patterning of the developing encephalic vesicles. Overall, *Hoxa2* activation in FNC cells resulted in atrophy of the fore- and midbrain, the downregulation of *Fgf8* in the ANR, isthmus and BA ectoderm, the downregulation of *Wnt8b*, and a lateral expansion of *Shh* expression.

Effect of *Hoxa2* on Bmp antagonists

We previously showed that the amounts of Bmp antagonists (*Gremlin* and *Noggin*) produced by FNC cells indirectly regulate *Fgf8* expression in the ANR. Surgical ablation of the FNC results in brain defects due to an increase in *Bmp* signaling in response to the loss of Bmp inhibitor production by the NC cells [10]. In normal development, *Noggin* is expressed in the migrating FNC cells responsible for populating the facial processes and BAs [28] (Fig. 1t; arrowheads). When *Hoxa2* expression was ectopically triggered in FNC cells, these cells displayed very low levels of *Noggin* expression in the maxillo-mandibular process (Fig. 1u; $n = 5$).

We analyzed the molecular profile of control and *Hoxa2*-transfected FNC embryos by PCR: the cephalic NC was surgically explanted after either sham or *Hoxa2*-RCAS transfection and grown in vitro for 24 h. PCR analyses demonstrated a loss of *Noggin* expression in *Hoxa2*-transgenic FNC (Fig. 1z). A similar effect on the expression of *Dan,* encoding another Bmp-antagonist produced by FNC cells [29, 30], was also found (Fig. 1z).

Effect of *Six2* silencing on gene expression in the developing head

Six2 has been shown to be a direct downstream target of *Hoxa2* in BA2, in which it is downregulated by the product of *Hoxa2* at specific sites [13]. *Six2* expression is observed in the developing head from 5ss onward, and is detected in migrating FNC cells as early as 10ss (Fig. S2a, b; arrowheads). At 25ss, *Six2* expression in FNC cells was detected in the vicinity of the trigeminal, facial and vestibulo-acoustic ganglionic anlagen, in the maxillo-mandibular processes and, to a lesser extent, in the naso-frontal bud (Fig. 1w; Fig. S2c–e). From this stage onwards, *Six2* expression became increasingly strong in the NC-derived mesenchyme and endodermal pouches (Fig. S2f, g).

In experimental embryos, ectopic *Hoxa2* activity prevented the expression of *Six2* in FNC-derived cells, but did not affect the expression of *Six2* in the pharyngeal endoderm (Fig. 1x; $n = 6$). Similarly, PCR analysis of *Hoxa2*-expressing NC cells grown in vitro confirmed the downregulation of *Six2* following transfection with *Hoxa2* (Fig. 1z).

We investigated the intrinsic role of *Six2* in head development by silencing the *Six2* gene in the FNC. We used the same method to transfect the FNC cells of 5–6ss embryos bilaterally with a dsRNA targeting *Six2*, and then transferring these cells into naive embryos (Fig. 1a). At E2.5, *Six2*-depleted embryos displayed severe facial hypoplasia and atrophy of the pre-otic brain. As described above, gene expression analyses in experimental embryos were performed by in situ hybridization and RT-PCR on explanted FNC cells. Both approaches confirmed the inhibition of *Six2* in FNC in vivo and in vitro (Fig. 1y, z). By contrast, the endodermal expression of *Six2* was unaffected after surgery.

Influence of *Six2* silencing on gene expression in the developing head

We analyzed the pattern of expression of the *Fgf8*, *Bmp4*, *Wnt8b*, and *Shh* genes in *Six2*-depleted embryos, at E2.5. The loss of *Six2* function in FNC cells modified *Fgf8* expression in a similar manner to *Hoxa2* transfection: *Fgf8* activity was inhibited in the ANR, the isthmus, and the BA1 ectoderm (Fig. 1j; $n = 5$). *Bmp4* transcript accumulation was maintained in the nasofrontal and maxillary regions (Fig. 1m). Following the silencing of *Six2*, a considerable expansion was observed in the domain of *Shh* expression in the pre-otic neuroepithelium, as in the *Hoxa2*-transfected embryos (Fig. 1p, arrowheads; $n = 6$), and an upregulation of *Shh* expression was observed in the maxillo-mandibular commissural ectoderm (asterisk). Similarly, along the prosencephalic and rhombencephalic midline, *Six2* silencing narrowed the region of *Wnt8b* expression (Fig. 1s; white arrowheads).

We then investigated the consequences of *Six2* silencing for the expression of genes encoding Bmp-antagonists: *Six2* inactivation led to the downregulation of both *Noggin* (Fig. 1v, z) and *Dan* (Fig. 1z).

Further head and brain development in *Six2*-silenced embryos

As the ectopic activation of *Hoxa2* in FNC severely compromised face and brain development [12], we looked for cerebral and skeletal defects after *Six2* depletion in FNC cells.

At E5, the cephalic vesicles of isolated brains from *Six2*-dsRNA-treated embryos exhibited major defects. The telencephalic vesicles were smaller than in controls: the dorsolateral development of the pallium, the thalamus, and the optic tectum were abnormal (Fig. 2a–d; $n = 5$). *Six2* silencing in the FNC also had detrimental effects on the development of the prosencephalic and rhombencephalic choroid plexi, which were totally disorganized (Fig. 2d, asterisk). More specifically, at prosencephalic level, the inhibition of *Six2* activity in FNC cells affected the development of the pallium and septum pellucidum, which were atrophied compared to the control (Fig. 2e, f). Similarly, the thalamus appeared underdeveloped (Fig. 2e, f).

Six2 loss-of-function in the FNC led to severe defects of head skeletal development at E8: the nasal septum and capsule were almost completely absent and the mandible was

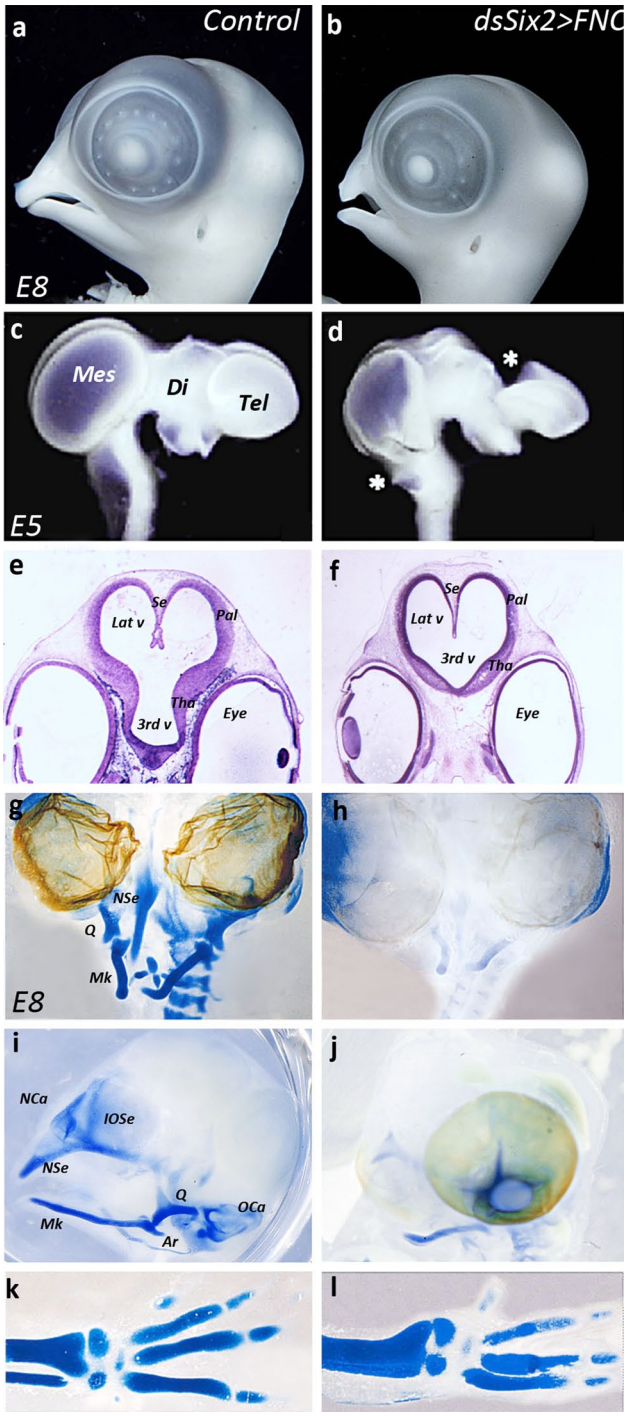

Fig. 2 *Six2*-silencing in the FNC hampers head and brain development. **a**, **b** Morphology and **c**, **d** whole-mount brain preparation in control (**a**, **c**) and experimental (**b**, **d**) embryos. In *Six2*-silenced embryos, the nasofrontal and maxillo-mandiblar development is atrophied (**b**), and brain morphology is altered along the dorsal midline (**d**): choroid plexi are missing (*stars*). *Cresyl-violet* staining of paraffin sections (**e**, **f**) on E5 control (**e**) and experimental (**f**) embryos showing the defective development of prosencephalic structures in experimental series: the pallial and thalamic neuroepithelium are thinner than in control (**f**). In addition, the inter-hemispheric septum fails to form normally. **g–j** Whole-mount staining of cartilage in the head skeleton of E8 (**g**, **i**) control and (**h**, **j**) *Six2*-silenced embryos. On frontal views (**g**, **h**), much of the nasal and mandibular cartilages are absent in experimental embryos (**h**). On profile views (**i**, **j**), the skeletal defects resulting from the silencing of *Six2* consist in the absence of the interorbitary and nasal septa, nasal and otic capsules, quadrate and articular (**j**); on control embryo, eyeballs have been removed to evidence skeletal structures at the midline. By contrast, the development of the appendicular skeleton is similar in the control and *Six2*-silenced series, as shown by the normal development of the radius, ulna, and digits (**k**, **l**). *Ar* articular, *Di* diencephalon, *IOSe* interorbital septum, *Lat v* lateral ventricle, *Mes* mesencephalon, *Mk* Meckel's cartilage, *NCa* nasal capsule, *NSe* nasal septum, *OCa* otic capsule, *Pal* pallium, *Q* quadrate, *Se* septum, *Tel* telencephalon, *Tha* thalamus, *3rd v* third ventricule

reduced in its distal-most part (Fig. 2g–j). Moreover, the articular, the quadrate, the interorbital septum, the sclera, and the otic capsule were totally missing (Fig. 2i, j). In contrast, the appendicular skeleton of *Six2*-depleted embryos developed normally (Fig. 2k, l).

Rescue of the *Hoxa2* phenotype by *Six2*

As *Six2* silencing reproduced the molecular and morphological changes induced by *Hoxa2* translocation, we tried to rescue the dysmorphologies generated by *Hoxa2* by cotransfection of *Hoxa2* and *Six2*. This experiment was performed by simultaneously transfecting FNC cells with *Hoxa2* and *Six2* retroviral constructs, in the same experimental design as for the preceding experiments. The embryos were observed at 24ss: the combined expression of *Six2* and *Hoxa2* led to normal head development (Fig. 3a–i; $n = 5$). Similarly, the gene expression pattern of *Fgf8*, *Wnt8b, Shh*, and *Noggin* tended to normalize when *Six2* was cotransfected with *Hoxa2* in FNC cells (Fig. S3; compare with Fig. 1i, o, r). These observations were confirmed by the analysis of the skeletal phenotype resulting from these experimental series at E8: while *Hoxa2* totally hampered the skeletal differentiation, cotransfection of *Hoxa2* and *Six2* in FNC cells fully restored the development of nasofrontal and maxillo-mandibular structures (Fig. 3j–l; $n = 3/3$). The elimination of the deleterious effects of *Hoxa2* expression by the upregulation of *Six2* revealed that *Six2* encodes a major transcription factor controlling the early steps of head development.

Involvement of *Six1* and *Six4* in head morphogenesis

As the cerebral and skeletal defects resulting from *Six2* silencing in the FNC did not amount to a full phenocopy of those resulting from *Hoxa2* activation, we searched for other genes from the same family that might serve as downstream targets of *Hoxa2* in the developing head. We investigated whether the transfection of FNC cells with *Hoxa2* affected the expression of *Six1* and *Six4*, both of

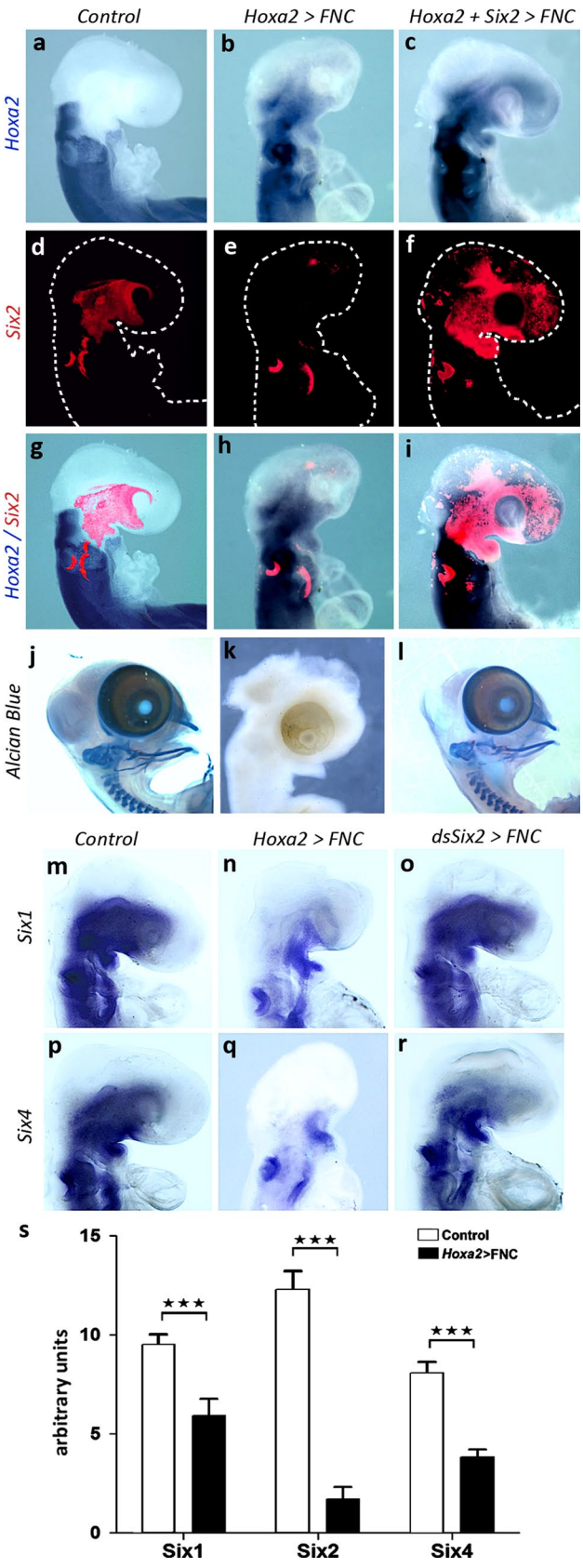

Fig. 3 Molecular interactions between *Hoxa2*, *Six2*, *Six1* and *Six4*. ▶ **a–c** *Hoxa2* expression in control, *Hoxa2*, and *Hoxa2*+*Six2* transgenic embryos: whole-mount in situ hybridizations show the expansion of *Hoxa2* transcript accumulation at the expense of facial territories in embryos engrafted with *Hoxa2*-transfected FNC (**b**, **c**). **d–f** *Six2* transcript accumulation evidenced by fluorescent hybridization (*red*) in the same embryos; embryos are delineated with *dotted lines*. The forced expression of *Hoxa2* in FNC cells inhibits the activity of *Six2* (**e**), which can be restored when *Hoxa2* and *Six2* are cotransfected in FNC cells (**f**). **g–i** Superimposed expression of *Hoxa2* and *Six2*: *Six2* overexpression in the FNC can rescue the *Hoxa2* phenotype at E2.5 (**i**). **j–l** Whole-mount skeletal preparation of control, *Hoxa2*, and *Hoxa2*+*Six2* transgenic embryos. *Alcian blue* staining shows the complete set of skeletal elements in controls at E8 (**j**). *Hoxa2* expression in FNC totally hampers skeletal differentiation at this stage (**k**), but cotransfection of *Hoxa2*+*Six2* fully restores the development of maxillo-facial and mandibular skeleton (**l**). **m–o** *Six1* and **p-r** *Six4* expression in (**m**, **p**) control, (**n**, **q**) *Hoxa2*-transfected, (**o**, **r**) dsSix2-transfected embryos. *Hoxa2* ectopic expression strongly affects the activity of *Six1* and *Six4* in FNC cells (**n**, **q**), while the silencing of *Six2* has a limited effect (**o**, **r**). **s** qRT-PCR analysis of *Six* gene activity on explanted FNC cells following *Hoxa2* transfection. Control FNC cells express high level of *Six1*, *Six2*, and *Six4*. After induction of *Hoxa2*, the activity of all of the three genes is strongly affected. ***$P < 0.001$. *Error bars* SEM from three independent experiments, which have been performed in triplicate

which are activated in FNC-derived mesenchyme. During normal development, *Six1* and *Six4* display similar patterns of expression at 24ss: transcripts are present in the maxillo-mandibular region, more caudal BAs, and in the otic vesicles (Fig. 3m, p). The ectopic activation of *Hoxa2* expression greatly reduced the expression of *Six1* and *Six4* in the maxillo-mandibular region (Fig. 3n, q). In contrast, *Six2* silencing in FNC cells slightly impacted on *Six1* and *Six4* expression pattern at 24ss (Fig. 3o, r).

In order to quantify the changes in *Six* gene expression resulting from the ectopic activation of *Hoxa*2 in the FNC, we performed a qRT-PCR analysis on control and *Hoxa2*-transfected FNC cells that were grown for 24 h in vitro before RNA preparation. The SYBR green assays were normalized on GAPDH activity. The quantification of gene expression revealed that *Hoxa2* chiefly affected the activity of *Six2*, which was significantly reduced when compared to control series ($Six2\Delta = 710$ %; Fig. 3s). Similarly, *Six1* and *Six4* expression activity shrank in *Hoxa2*-transfected FNC cells ($Six1\Delta = 78$ %, $Six4\Delta = 110$ %; Fig. 3s).

We explored the respective roles of *Six1* and *Six4* genes in brain development by selectively modifying the expression of these two genes through dsRNA-driven gene silencing at 5–6ss followed by functional screening of effects on the morphogenesis of cephalic vesicles at E5. *Six1* silencing in FNC cells entailed profound changes in brain development with respect to the control (Fig. 4a–d). Structural defects in *Six1*-depleted embryos consisted in a dramatic

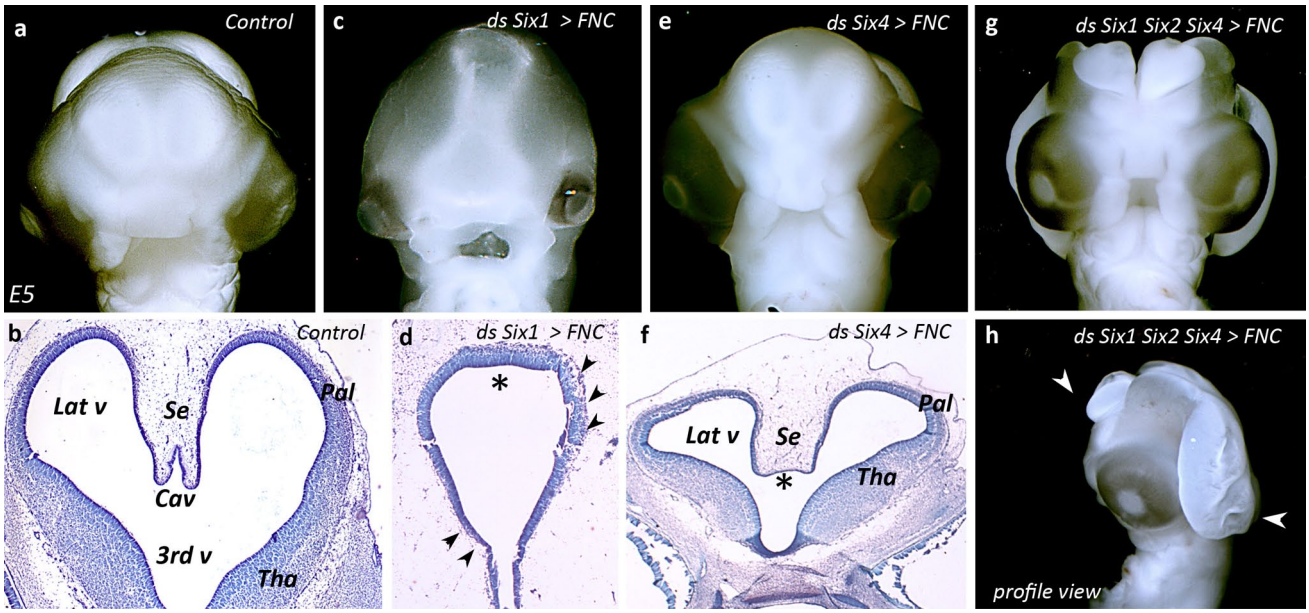

Fig. 4 Silencing of *Six* gene impairs brain development. **a–l** Analysis of brain development in E5 (**a–c**) control, (**d–f**) *Six1*-, (**g–i**) *Six4*-, (**j–l**) *Six1/Six2/Six4*-silenced embryos. At this stage, in control embryos (**a**), the telencephalic hemispheres are well developed (**b**). **c**, **d** Knocking-down *Six1* in FNC cells hampers the development of pallial and subpallial structures (**d**, *arrowheads*) and inhibits the septation of the anterior prosencephalon (**d**, *asterisk*). **e**, **f** Inhibition of *Six4* results in mild defects, which affect the formation of the septum pellucidum (**f**, *asterisk*). The triple silencing degenerates towards a dramatic anencephaly (**g**), which extends from the telencephalon down to the anterior rhombencephalon (**h**, *arrowheads*). *Cav* cavum pellucidum, *Lat v* lateral ventricle, *Pal* pallium, *Se* septum pellucidum, *Tha* thalamus, *3rd v* third ventricle

microcephaly (Fig. 4c). The telencephalic septation failed to form, and embryos virtually exhibited an alobar holoprosencephaly together with a severe atrophy of the prosencephalic neuroepithelium (Fig. 4d; asterisk and arrowheads). In contrast, depriving FNC cells of *Six4* activity resulted in a different outcome. The cephalic vesicles were smaller than normal (Fig. 4e, f). Notably, the diverticulation of the anterior primitive prosencephalon occurred: the cerebral hemispheres and the lateral ventricles formed. However, in these embryos, the inter-hemispheric septum was broader than normal and the cavum failed to develop (Fig. 4f; asterisk).

In order to further analyze the requirement of *Six* gene activity in FNC cells for brain development, we decided to silence the three genes, *Six1*, *Six2*, and *Six4*, simultaneously in FNC cells at 5–6ss. At E5, the triple silencing generated a dramatic anencephalic condition (Fig. 4g). Embryos exhibited a profound brain defect that encompassed the tel-, di-, and mesencephalon (Fig. 4h; arrowheads). Such a phenotype was reminiscent of that resulting from either FNC ablation or *Hoxa2* activity in FNC [12], hence pointing to the requirement of *Six* gene activity in the *Hox*-negative NC for the proper development of the pre-otic brain.

Later on, we also examined the impact of *Six1* and *Six4* loss-of-function on craniofacial development at E8. Embryos subjected to *Six1* downregulation displayed no loss of skeletal elements with respect to the control (Fig. 5a–c). However, *Six1* silencing strongly affected facial cartilage size, leading to a global homothetic decrease in the size of the head skeleton (Fig. 5d–f). This phenotype was different from that resulting from the silencing of *Six4*. At E8, embryos subjected to *Six4* silencing displayed a striking skeletal phenotype (Fig. 5g–i). All but the proximal and distal tips of the nasofrontal and mandibular cartilages were missing; the remaining skeletal structures, part of the quadrate, the rostral end of Meckel's cartilages, the nasal septum, and the entoglossum were all smaller than normal (Fig. 5h, i).

Pursuing the idea that ectopic *Hoxa2* activity might inhibit the expression of *Six1*, *Six2*, and *Six4*, we decided to switch off the expression of all three of these genes simultaneously, by electroporating FNC cells with dsRNA molecules targeting these three genes at 5–6ss. At E8, the triple silencing of *Six1*, *Six2*, and *Six4* completely prevented skeletogenic differentiation (Fig. 5j–l; $n = 5/5$). None of the elements of the facial skeleton developed (Fig. 5j) and whole-mount skeletal preparations were totally transparent (Fig. 5k, l), mimicking the skeletal phenotype resulting from the transfection of FNC cells with *Hoxa2* [12].

Thus, the various *Six* genes involved in head skeletogenesis have different, complementary roles in this process, suggesting that craniofacial skeletogenesis, which normally

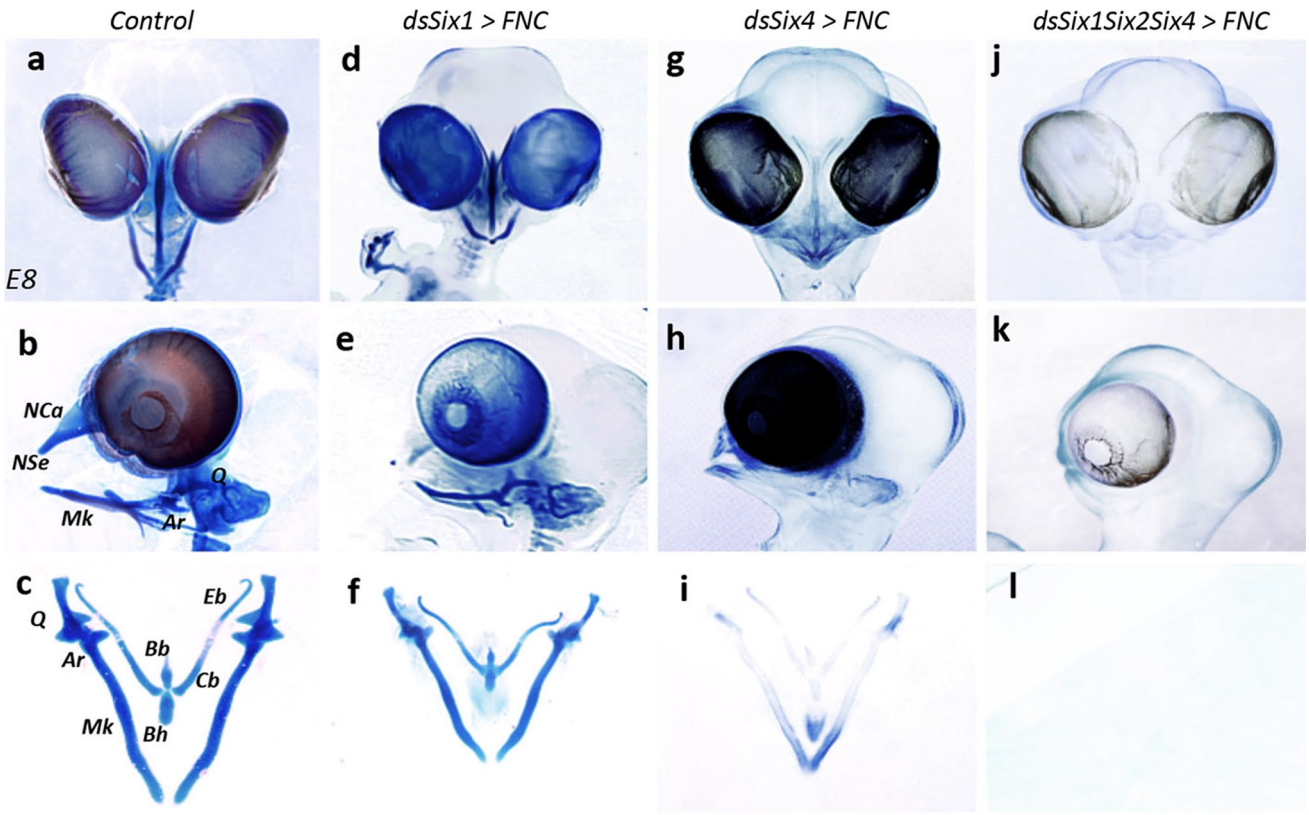

Fig. 5 *Six* genes have complementary role in head skeletogenesis. **a–l** Skeletal preparation of E8 (**a–c**) control, (**d–f**) *Six1*-, (**g–i**) *Six4*-, (**j–l**) *Six1/Six2/Six4*-silenced embryos. The genes *Six1* and *Six4* genes, when knocked-down, generate different skeletal phenotypes. The phenotype resulting from the triple silencing of *Six1/Six2/Six4* sums up the requirement of each targeted gene for skeletal development and reveals their complementary role in the skeletogenic patterning. *Ar* articular, *Bb* basibranchial, *Bh* basihyal, *Cb* ceratobranchial, *Eb* epibranchial, *Mk* Meckel's cartilage, *NCa* nasal capsule, *NSe* nasal septum, *Q* quadrate

takes place in a Hox-free domain, closely depends on the combinatorial expression of *Six* genes for growth and patterning.

Relationship between *Six* genes and *Noggin* expression in the FNC

As mentioned above, the adverse effects of *Hoxa2* activity in the FNC were accompanied by the downregulation of Bmp antagonists. We therefore hypothesized that *Hoxa2* expression might exert its negative effects on face and brain development by interfering with the regulation of Bmp signaling. We decided to counteract the effects of *Hoxa2* through the forced expression of *Noggin* in the same system. FNC cells were cotransfected with retroviral constructs driving the expression of *Hoxa2* and *Noggin* at 5–6ss. As previously indicated, the electroporated tissue was subsequently transplanted into a naive recipient embryo (see Fig. 1a). We first investigated whether *Noggin* overexpression could restore normal levels of *Six2* expression. We found that *Hoxa2* expression completely prevented *Six2* gene activity in the developing head (Fig. 6a, b), and that the overexpression of *Noggin* and *Hoxa2* together did not rescue *Six2* activity in the FNC-derived mesenchyme (Fig. 6c). However, even in the absence of *Six2* activity, the forced expression of *Noggin* induced a significant restoration of normal head development (Fig. 6c; $n = 7/7$). We investigated the cellular events accounting for these morphological changes by studying cell proliferation and death in parallel in control, *Six2*-depleted, *Hoxa2*, and *Hoxa2* + *Noggin* transgenic embryos at 18ss, on frontal views (Fig. 6d–l). In control embryos, particularly high levels of cell proliferation were detected by PhH3 immunolabeling in the dorsal parts of the prosencephalic and optic vesicles, and in BA1 (Fig. 6d). Cell death was observed only rarely, rostrally and mostly along the anterior midline, at the level of the ANR (Fig. 6e). By contrast, both *dsSix2* ($n = 5/5$) and *Hoxa2*-treated ($n = 10/10$) embryos displayed much lower levels of cell proliferation, particularly in the dorsolateral areas (Fig. 6f, h; green arrows). In these embryos, the territory in which cell death occurred was larger, encompassing much of the prosencephalic territory along with the lateroventral part of the diencephalon and the optic stalk (Fig. 6g, i; red arrows). In addition, the

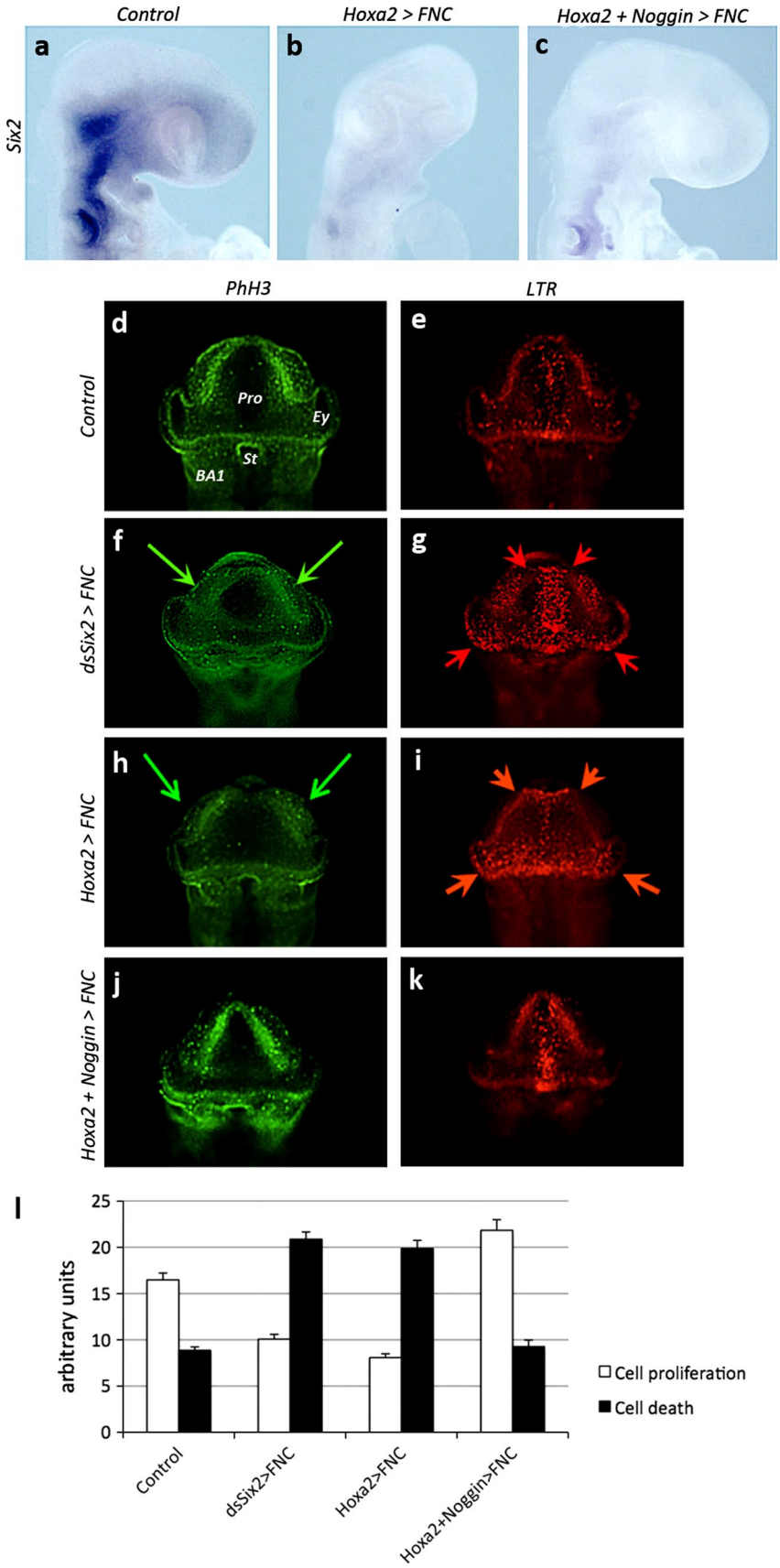

Fig. 6 Noggin supplementation in *Hoxa2*-treated embryos can bypass *Six* inhibition to restore cell proliferation and reduce cell death. **a**–**c** Comparison for *Six2* expression between (**a**) control, (**b**) *Hoxa2*, and (**c**) *Hoxa2*+*Noggin* transgenic embryos at E2. *Hoxa2* represses *Six2* expression (**b**), but *Noggin* can restore normal facial development (**c**). Analysis of (**d**, **f**, **h**, **j**) cell proliferation through PhH3 immunodetection and (**e**, **g**, **i**, **k**) cell death by whole-mount LTR staining in (**d**, **e**) control, (**f**, **g**) *dsSix2*-treated, (**h**, **i**) *Hoxa2*, and (**j**, **k**) *Hoxa2*+*Noggin*-tranfected embryos. *Hoxa2* activity in FNC cells early biases cell proliferation and death in the developing head towards a deleterious condition. **l** Quantification of cell proliferation and death in control and experimental series. Supplementation with *Noggin* tends to normalize the balance between cell proliferation and death. *BA1* 1st branchial arch, *Ey* eye, *Pro* prosencephalon, *St* stomodeum

expansion of cell death along the dorsal midline was associated with the initiation of brain defects (Fig. 6g, i). When *Hoxa2* expression was combined with *Noggin* expression, cell proliferation patterns tended to normalize (Fig. 6j, l). Additionally, cell death was reduced and occurred only in the very anterior midline (Fig. 6k, l; $n = 12/12$). The effects of *Noggin* on head development in the presence of ectopic *Hoxa2* activity could therefore be attributed to both an increase in proliferation and lower levels of cell death.

Noggin can rescue the effects of *Hoxa2*

As *Noggin* activity in the migrating FNC cells was demonstrated to be critical for encephalization, through the control of Fgf8 production in the ANR, we explored the regulation of *Fgf8* activity in these series. The forced expression of *Hoxa2* in FNC cells resulted in much lower levels of *Fgf8* transcripts in the ANR and isthmus (Fig. 7a, b). Following the cotransfection of FNC cells with both *Noggin* and *Hoxa2*, Noggin activity prevented the effects of *Hoxa2* and normalized *Fgf8* activity in the ANR, isthmus, and BAs (Fig. 7c; $n = 6/6$). We investigated the effect of this treatment on brain development. Isolated brain preparations from E4 embryos revealed normal development of the pre-otic encephalic vesicles, with morphological subdivisions into telencephalic hemispheres, thalamus, and optic tectum (Fig. 7d). In E4 embryos transfected with *Hoxa2* alone, the dorsal part of the brain was missing, such that the cephalic vesicles were no longer recognizable (Fig. 7e). By contrast, transfection with both *Hoxa2* and *Noggin* restored brain development to normal morphology (Fig. 7f).

We investigated whether *Noggin* expression could counteract the effects of *Hoxa2* on facial skeletogenesis, by assessing the expression of *Sox9*, a master gene of chondrogenesis [31], in control, *Hoxa2*, and *Hoxa2* + *Noggin* transgenic embryos at E5. In control embryos, *Sox9* was homogeneously expressed throughout the facial processes, including the nasofrontal region, as well as in the maxillary and mandibular buds (Fig. 7g, j). But its expression was strongly downregulated in *Hoxa2*-transfected embryos (Fig. 7h, k; arrowheads). *Noggin* overexpression restored *Sox9* expression in the developing face (Fig. 7i, l). These results were further confirmed by a qRT-PCR analysis performed on in vitro experiments. According to the paradigm previously evoked, FNC cells taken from control, *Hoxa2*-transfected, and *Hoxa2* + *Noggin* cotransfected embryos were grown for 24 h in vitro before harvesting RNA. The quantification of *Sox9* gene expression revealed that *Hoxa2* reduced its activity ($Sox9\Delta = -67.53$ %; Fig. 7m). In contrast, in *Hoxa2* + *Noggin*-cotransfected FNC cells, *Sox9* activity was restored to the level of control series ($Sox9\Delta = 21.93$ %; Fig. 7m).

Fig. 7 *Noggin* expression can overcome the deleterious effects of *Hoxa2* on brain and skeletal development. Comparisons between (**a**, **d**, **g**, **j**, **m**) control, (**b**, **e**, **h**, **k**, **n**) *Hoxa2*, (**c**, **f**, **i**, **l**, **o**) *Hoxa2*+*Noggin* transgenic embryos (**a**–**c**) in *Fgf8* expression, (**d**–**f**) E4 brain morphology, (**g**–**l**) E5 *Sox9* expression. Supplementation of *Hoxa2*-treated embryos with *Noggin* can restore the effect of *Hoxa2* on *Fgf8* activity in ANR, BAs and isthmus (**b**, **c**). Under this condition, the brain development, which is severely compromised by *Hoxa2* (**e**), is restored and the cephalic vesicles of the fore- and midbrain develop (**f**). **g**–**i** At E5, whole-mount hybridization for *Sox9* shows that *Noggin* activity can counterbalance the inhibition of *Sox9* expression by *Hoxa2* to control the chondrogenic commitment of FNC cells. On paraffin sections (**j**–**l**), the mesenchyme in the maxillo-mandibular processes normally expresses *Sox9* (**j**); *Hoxa2* inhibits its expression (**k**), but *Noggin* can restore the chondrogenic potential of mesenchymal cells by stimulating *Sox9* activity (**l**). **m** qRT-PCR analysis performed on FNC cells subjected to normal condition, *Hoxa2*-, and *Hoxa2*+*Noggin*-transfection and grown in vitro for 24 h, shows that *Hoxa2* represses *Sox9* activity, but *Noggin* can overcome its effect. *Error bars* SEM from three independent experiments, which have been performed in triplicate (***$P < 0.001$). **n**–**p** *Alcian blue* staining of whole-mount skeletal preparation of control, *Hoxa2* and *Hoxa2*+*Noggin* transgenic embryos. The skeletal development at E8 (**n**), which is completely abolished by *Hoxa2* (**o**), is restored by *Noggin* (**p**). **q**, **r** *Alcian blue* and *alizarin red* staining of skeletal preparation at E10 Similarly, when Noggin is cotransfected with the three dsRNA against *Six1*, *Six2*, and *Six4*, its activity is sufficient to fully restore skeletogenic development (**r**). *Md* mandibular bud, *Mx* maxillary process, *OTe* optic tectum, *Pal* pallium, *T* tongue, *Tha* thalamus

These observations suggested that Noggin might rescue skeletogenesis in *Hoxa2*-transfected FNC cells. Skeletogenic phenotypes were analyzed on whole-mount skeletal preparations at E8. Alcian blue staining showed a normal pattern for the facial skeleton in control embryos (Fig. 7n), whereas the facial skeleton was totally missing in *Hoxa2*-transgenic embryos (Fig. 7o; $n = 9/9$). The entire set of skeletal elements corresponding to the upper face (the nasal capsule and septum) and lower jaw (Meckel's cartilage, the quadrate, and entoglossum) was restored by the overexpression of *Noggin,* which counteracted the effects of *Hoxa2* in FNC cells (Fig. 7p; $n = 5/5$).

In order to see whether the activity of *Noggin* is downstream of *Six* genes' activity, we tried to rescue the lack of skeletal development resulting from the triple silencing of *Six1*, *Six2*, and *Six4* (Fig. 5k, l) by cotransfecting the three dsRNA with the retroviral construct driving *Noggin* expression. At E10, we observed the complete restoration of the skeletal nasofrontal and maxillo-mandibular structures (Fig. 7q, r). These results therefore showed that the control of head morphogenesis operated by the combination of *Six* genes is mediated by *Noggin* activity.

Discussion

In this work, we explored the molecular mechanisms by which *Hoxa2* expression affects the developmental program

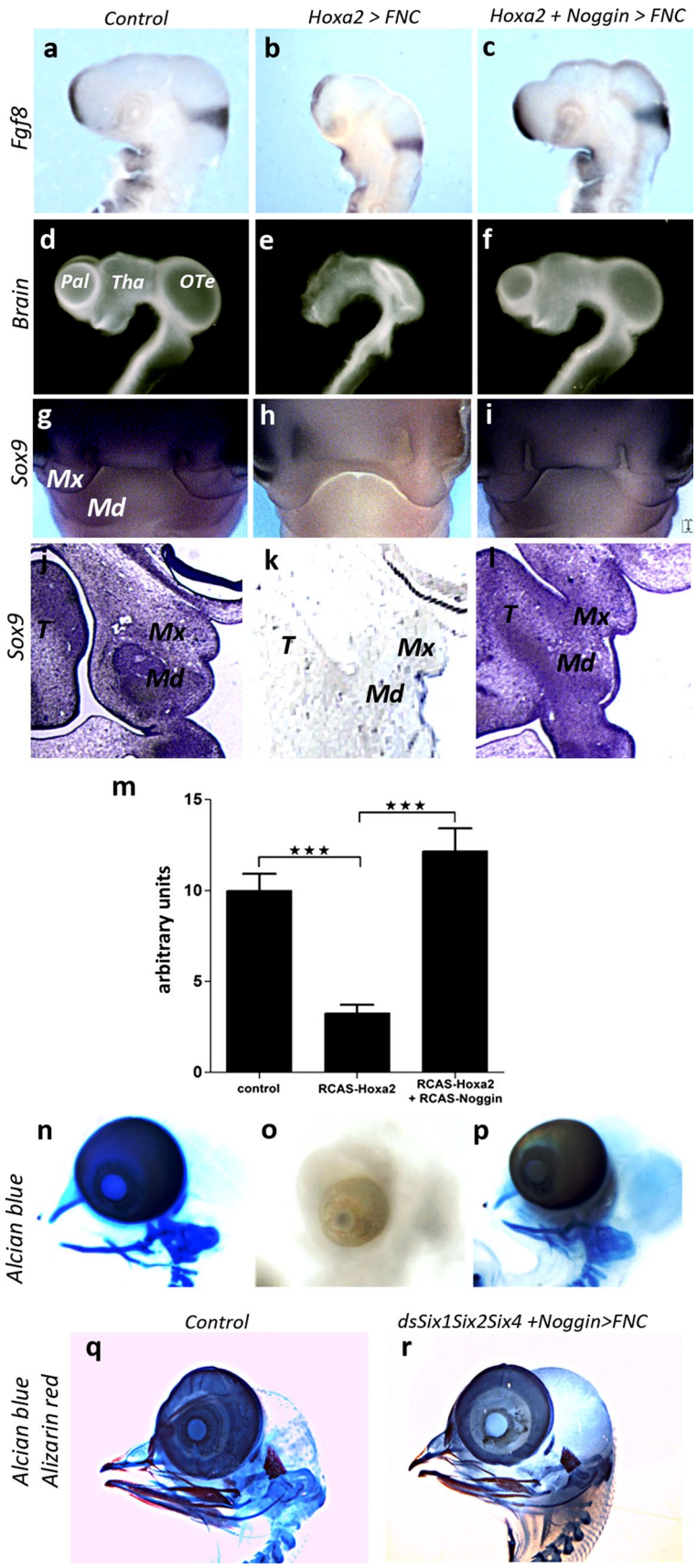
Control
Hoxa2 > FNC
Hoxa2 + Noggin > FNC
Fgf8
Brain
Sox9
Sox9
Alcian blue
Alcian blue
Alizarin red
a
b
c
d
e
f
g
h
i
j
k
l
m
n
o
p
q
r
Pal
Tha
OTe
Mx
Md
T
arbitrary units
control
RCAS-Hoxa2
RCAS-Hoxa2
+ RCAS-Noggin
dsSix1Six2Six4 +Noggin>FNC

of the FNC, preventing the development of both facial structures and pre-otic brain. Most of the adverse effects of *Hoxa2* expression in the FNC on the development of the facial skeleton and brain were reproduced by the inhibition of *Six2* expression in the NC-derived mesenchyme. The *Six2* gene, which is a direct target of Hoxa2 in BA2 [13, 32], is strongly expressed in the Hox-free NC cells from the beginning of their migration until E5, the last time point recorded in our observations. When *Hoxa2* expression is triggered in the normally Hox-free cephalic neural fold, which gives rise to the facial and cranial skeleton and connective tissue, NC cells lose their ability to express *Six2*. In parallel, we showed that *Six2* silencing resulted in the loss of much of the NC-derived head skeleton and profound abnormalities of brain development, such as defects of the dorsal pre-otic structures, which develop from the alar plate anlage of the anterior neural plate. These defects, evident from E2 onwards, are consistent with the dorsalizing effect of the migrating FNC cells on the development of the cephalic vesicles as already demonstrated [6, 10]. In particular, *Hoxa2* activation or *Six2* inactivation caused the loss of *Fgf8* and *Wnt8b* expression. The molecular change in *Fgf8* expression in the ANR due to the repression of *Noggin* expression in the migrating FNC cells, as observed in both situations, had a profound impact on the development of the prosencephalon and mesencephalon. Similarly, changes of the pattern of *Wnt8b* gene expression preceded alterations of choroid plexus development.

The parts of the brain that turn out to mostly depend on the regulatory activity of the FNC are those that have evolved more recently: the telencephalon and the dorsal part of the di- and mesencephalon. We show here that the development of these structures is incompatible with the expression of genes of the *Hox* clusters, which pattern the rest of the body plan in all Bilateria. Furthermore, the lack of choroid plexus formation after transfection with *Hoxa2* or *Six2* silencing suggests that the development of these essential structures for brain homeostasis benefits from the input of the FNC via *Six* gene activity.

Two other *Six* genes in addition to *Six2* were found to be essential for head development. Despite their overlapping patterns of expression in premigratory and migrating NC cells, silencing of *Six1*, *Six2*, and *Six4* in FNC cells had detrimental effects that were differently distributed on the head structures. As far as brain morphogenesis is concerned, each *Six* gene when separately switched off through RNAi exerts a complementary role in patterning the dorsal midline of the pre-otic brain: *Six2* silencing results in the loss of the choroid plexus at both prosencephalic and rhombencephalic levels, while *dsSix4* perturbs the formation of the septum pellucidum, a condition reminiscent of lobar holoprosencephaly, and *dsSix1* affects the diverticulation of the prosencephalon, hence leading to a flagrant alobar holoprosencephaly. So, individually, *Six1*, *Six2*, and *Six4* genes cannot reciprocally compensate their effect on brain development for the loss of the others. The phenotype resulting from the triple silencing gives rise to a severe anencephaly, a worsened condition, which recapitulates all the defaults mentioned above, and phenocopies the activation of *Hoxa2*. Altogether, these data point to the complementary role of *Six* gene expression in the FNC for the proper development of the brain.

Regarding the facial skeleton, *Six2* silencing selectively hampered nasofrontal skeleton, joint, and mandibular symphysis development, but had no effect on development of the medial part of Meckel's cartilage. *Six1* silencing resulted in an overall homothetic reduction of the head skeleton and *Six4* silencing, specifically targeted the nasofrontal and mandibular skeleton, but had no effect on proximal and distal structures. The simultaneous silencing of all three genes completely prevented skeletal development. Our data therefore demonstrate the synergistic roles of the *Six1*, *Six2*, and *Six4* genes, which cooperate to provide the scaffolding of craniofacial structures (Fig. S4). The ectopic expression of *Hoxa2* thus reveals a requirement for *Six* genes for the spatial layout of skeletogenic NC derivatives.

Recently, the mutation of a chromatin-remodeling gene, *Cecr2*, has been associated with neural tube defects and facial abnormalities, the severity of which depends on the genetic background. This mutation affects much of the genes early expressed by the FNC cells, among which is *Six1* [33]. These data strongly suggest that the activity of *Six* gene in FNC cells can be epigenetically regulated; such a mechanism could account for the congenital malformations altering face and brain development, and deserves to be further explored.

Six genes have been conserved throughout evolution and encode transcription factors that can function either as transcription activators or repressors. *Six* homologs (*Sine oculis*, *Optrix*, and *DSix4*) in embryos were initially shown to play a role in eye development, through mutations in fly [34]. The ontogenetic importance of this gene family was subsequently documented for thymic and kidney morphogenesis and for muscle development in mammals [18]. These genes were shown to be essential for the ontogeny of all sense organs [35, 36]. In *Brachyrrine* (*Br*) mutants, generated by irradiation, the transcriptional repression of *Six2* is associated with frontonasal dysplasia and renal hypoplasia. In homozygous *Br/Br* mutants, despite the abolition of *Six2* expression throughout the body, only the facial skeleton was affected [37]. Thus, the mechanisms regulating bone and cartilage development is different in the head and trunk.

In our experiments, the forced expression of *Six2* in the FNC cells of embryos transfected with *Hoxa2* competitively overcame the adverse effects of *Hoxa2*

expression, restoring the competence of FNC cells for cephalic development. These observations are consistent with the results of genetic manipulations of BA2 development: *Hoxa2* knockout has been shown to expand the skeletogenic program in BA2 [38–41], leading to the development of BA1-like structures from BA2 territories in which *Six2* expression was relieved of *Hoxa2* activity. Furthermore, *Six2* overexpression confers on BA2 cells an ability to form BA1-like structures in a spatially restricted manner. Similarly, *Six2* overexpression in BA2 results in a phenocopy of *Hoxa2* inactivation. This indicates that, in normal BA2 development, *Hoxa2* switches off *Six2* expression in rhombencephalic NC cells [13, 32]. Concomitantly, *Hoxa2* represses the activation of *Pitx1* transcription by Fgf8 from the ectoderm, preventing the initiation of a "pro-mandible" program and restricting the domain of activation of *Sox9* and *Cbfa1*, two transcription factors essential for chondrogenic and membranous bone differentiation, respectively [42, 43]. Thus, *Six* gene expression in the developing head is essential, to drive the formation of craniofacial structures derived from the Hox-free domain of the NC, and to counteract the effect of the *Hox* genes involved in the patterning of pharyngeal structures.

Our experiments show that the treatment of FNC cells, by either *Hoxa2* activation or silencing of its downstream *Six* gene targets, results in an upregulation of Bmp signaling mediated by the loss of Bmp antagonists. In both cases, the upregulation of Bmp signaling is achieved through a decrease in *Noggin* and *Dan* production by FNC cells. Bmps decrease the amount of Fgf8 produced by the secondary brain organizers (ANR and isthmus) and BA1 ectoderm. The BA1 ectoderm is an important signaling center for the development of the jaw [5, 43, 44], whereas the ANR and isthmus are critical for brain development [6, 7, 11]. Thus, *Hoxa2* expression affects the development not only of the head skeleton but also of the telencephalon, thalamus, and optic tectum. The major role of anti-Bmp signaling by NC cells is further demonstrated by the abolition of the adverse effect of *Hoxa2* expression on Fgf8 production by the cotransfection of FNC cells with *Noggin*. Under this condition, forcing the expression of *Noggin* bypasses the inactivation of *Six*-gene pathway to rescue Fgf8 activity (Fig. S5). Such a restoration of normal development results from intense proliferation in the dorsal neuroepithelium and the limitation of cell death at the anterior midline, leading eventually to the normalization of cephalic vesicle development.

Noggin overexpression in *Hoxa2*-transfected embryos also causes a striking restoration of head skeleton development. In these experiments, the total absence of skeleton formation due to *Hoxa2* expression, mediated by the potent repression of *Sox9* expression, was reversed (Fig. S5). In this case, the entire set of skeletal structures was formed, owing to the restoration of *Sox9* activity.

In conclusion, the production by Hox-negative FNC cells of Bmp antagonists, under the control of *Six* genes, appears to be a key mechanism regulating head morphogenesis in vertebrates.

Acknowledgments We thank Dr. Françoise Dieterlen for critical reading of the manuscript, Drs. Andréa Trentin and Jörg Kobarg for the technical help with qRT-PCR, Drs. Brickell, Monsoro-Burq, Dressler, Oliver, and Niswander for providing plasmids. This work was supported by the Centre National de la Recherche Scientifique, and grants from the Agence Nationale de la Recherche (ANR-BLAN–0153) and the Ecole des Neurosciences de Paris (Réseau Technologique de Recherche Avancée:-Stem Cells). R.C.G. held fellowships from Fondation des Treilles, Egide, Conselho Nacional de Desenvolvimento Científico e Tecnológico/Coordenação de Aperfeiçoamento de Pessoal de Nível Superior (CNPq/CAPES—Brazil).

References

1. Gans C, Northcutt RG (1983) Neural crest and the origin of vertebrates: a new head. Science 20:268–274. doi:10.1126/science.220.4594.268
2. Hall BK (1998) Germ layers and the germ-layer theory revisited: primary and secondary germ layers, neural crest as a fourth germ layer, homology, and demise of the germ-layer theory. Evol Biol 30:121–186
3. Le Douarin NM (1982) The neural crest. Cambridge University Press, Cambridge
4. Le Douarin NM, Kalcheim C (1999) The neural crest, 2nd edn. Cambridge University Press, Cambridge
5. Creuzet S, Schuler B, Couly G, Le Douarin NM (2004) Reciprocal relationships between Fgf8 and neural crest cells in development. Proc Natl Acad Sci USA 101:4843–4847. doi:10.1073/pnas.0400869101
6. Creuzet SE, Martinez S, Le Douarin NM (2006) The cephalic neural crest exerts a critical effect on forebrain and midbrain development. Proc Natl Acad Sci USA 103:1433–1438. doi:10.1073/pnas.0605899103
7. Shimamura K, Rubenstein JL (1997) Inductive interactions direct early regionalization of the mouse forebrain. Development 124:2709–2718 ISSN: 0950–1991
8. Martinez S, Crossley PH, Cobos I, Rubenstein JLR, Martin GR (1999) FGF8 induces formation of an ectopic isthmic organizer and isthmocerebellar development via a repressive effect on Otx2 expression. Development 126:1189–1200 ISSN: 0950–1991
9. Echevarría D, Vieira C, Gimeno L, Martínez S (2003) Neuroepithelial secondary organizers and cell fate specification in the developing brain. Brain Res Rev 43:179–191. doi:10.1016/j.brainresrev.2003.08.002
10. Creuzet SE (2009) Regulation of pre-otic brain development by the cephalic neural crest. Proc Natl Acad Sci USA 106:15774–15779. doi:10.1073/pnas.0906072106
11. Ohkubo Y, Chiang C, Rubenstein JLR (2002) Coordinate regulation and synergistic actions of BMP4, SHH and FGF8 in the rostral prosencephalon regulate morphogenesis of the telencephalic and optic vesicles. Neuroscience 111:1–17. doi:10.1016/S0306-4522(01)00616-9
12. Creuzet S, Couly G, Bennaceur S, Vincent C, Le Douarin NM (2002) Negative effect of hox gene expression on the development of the neural crest-derived facial skeleton. Development 129:4301–4313 ISSN: 0950–1991

13. Kutejova E, Engist B, Mallo M, Kanzler B, Bobola N (2005) *Hoxa2* downregulates *Six2* in the neural crest-derived mesenchyme. Development 132:469–478. doi:10.1242/dev.01536
14. Le Douarin N, Dieterlen-Lièvre F, Creuzet S, Teillet M-A (2008) Quail—chick transplantations. Methods Cell Biol 87:19–58. doi:10.1016/S0091-679X(08)00202-1
15. Grapin-Botton A, Bonnin M-A, McNaughton LA, Krumlauf R, Le Douarin NM (1995) Plasticity of transposed rhombomeres: *Hox* gene induction is correlated with phenotypic modifications. Development 121:2707–2721 ISSN: 0950–1991
16. Pekarik V, Bourikas D, Miglino N, Joset P, Stoekli E (2003) Screening for gene function in chicken embryo using RNAi and electroporation. Nat Biotech 21:93–96. doi:10.1038/nbt770
17. Stoeckli ET (2003) RNAi in avian embryos. In RNAi: a guide to gene silencing, 297–312. Cold Spring Harbor Laboratory, New York. ISBN 978-087969704-4
18. Self M, Lagutin OV, Bowling B, Hendrix J, Cai Y, Dressler GR, Oliver G (2006) Six2 is required for suppression of nephrogenesis and progenitor renewal in the developing kidney. EMBO J 25:5214–5228. doi:10.1038/sj.emboj.7601381
19. Petrovová E, Sedmera D, Míšek I, Lešník F, Luptáková L (2009) Bendiocarbamate toxicity in the chick embryo. Folia Biol (Praha) 55:61–65 ISSN: 0015–5500
20. Henrique D, Adam J, Myat A, Chitnis A, Lewis J, Ish-Horowicz D (1995) Expression of a delta homologue in prospective neurons in the chick. Nature 375:787–790. doi:10.1038/375787a0
21. Crossley PH, Martinez S, Martin GR (1996) Midbrain development induced by FGF8 in the chick embryo. Nature 380:66–68. doi:10.1038/380066a0
22. Riddle RD, Johnson RL, Laufer E, Tabin CJ (1993) *Sonic hedgehog* mediates the polarizing activity of the ZPA. Cell 25:1401–1416. doi:10.1016/0092-8674(93)90626-2
23. Francis PH, Richardson MK, Brickell PM, Tickle C (1994) Bone morphogenetic proteins and a signaling pathway that controls patterning in the developing chick limb. Development 120:209–218 ISSN: 0950–1991
24. Connolly DJ, Patel K, Cooke J (1997) Chick noggin is expressed in the organizer and neural plate during axial development, but offers no evidence of involvement in primary axis formation. Int J Dev Biol 41:389–396 ISSN: 0214–6282
25. Garda AL, Puelles L, Rubenstein JLR (2002) Expression patterns of Wnt8b and Wnt7b in the chicken embryonic brain suggest a correlation with forebrain patterning centers and morphogenesis. Neuroscience 113:689–698. doi:10.1016/S0306-4522(02)00171-9
26. Pfaffl MW (2001) A new mathematical model for relative quantification in real-time RT-PCR. Nucl Acids Res 29:e45. doi:10.1093/nar/29.9.e45
27. Lako M, Lindsay S, Bullen P, Wilson DI, Robson SC, Strachan T (1998) A novel mammalian Wnt gene, WNT8B, shows brain-restricted expression in early development, with sharply delimited expression boundaries in the developing forebrain. Hum Mol Gen 7:813–822. doi:10.1093/hmg/7.5.813
28. Tzahor E, Kempf H, Mootoosamy RC, Poon AC, Abzhanov A, Tabin CJ, Dietrich S, Lassar AB (2003) Antagonists of Wnt and BMP signaling promote the formation of vertebrate head muscle. Gen Dev 17:3087–3099. doi:10.1093/hmg/7.5.813
29. Hsu DR, Economides AN, Wang X, Eimon PM, Harland RM (1998) The *Xenopus* dorsalizing factor gremlin identifies a novel family of secreted proteins that antagonize BMP activities. Mol Cell 1:673–683. doi:10.1016/S1097-2765(00)80067-2
30. Eimon PM, Harland RM (2001) *Xenopus* dan, a member of the dan gene family of BMP antagonists, is expressed in derivatives of the cranial and trunk neural crest. Mech Dev 107:187–189. doi:10.1016/S0925-4773(01)00462-2
31. Wright E, Hargrave MR, Christiansen J, Cooper L, Kun J, Evans T, Gangadharan U, Greenfield A, Koopman P (1995) The Sry-related gene *Sox9* is expressed during chondrogenesis in mouse embryos. Nat Genet 9:15–20. doi:10.1038/ng0195-15
32. Kutejova E, Engist B, Self M, Oliver G, Kirikenko P, Bobola N (2008) *Six2* functions redundantly immediately downstream of *Hoxa2*. Development 135:1463–1470. doi:10.1242/dev.017624
33. Fairbridge NA, Nicholas A, Dawe CE, Niri FH, Kooistra MK, King-Jones K, McDermid HE (2010) Cecr2 mutations causing exencephaly trigger misregulation of mesenchymal/ectodermal transcription factors. Birth Def Res A 88:619–625. doi:10.1002/bdra.20695
34. Kumar JP (2009) The sine oculis homeobox (*SIX*) family of transcription factors as regulators of development and disease. Cell Mol Life Sci 66:565–583. doi:10.1007/s00018-008-8335-4
35. Christophorou NA, Bailey AP, Hanson S, Streit A (2009) Activation of *Six1* target genes is required for sensory placode formation. Dev Biol 336:327–336. doi:10.1016/j.ydbio.2009.09.025
36. Suzuki Y, Keiko I, Kawakami K (2011) Development of gustatory papilla in the absence of *Six1* and *Six4*. J Anat 219:710–721. doi:10.1111/j.1469-7580.2011.01435.x
37. Fogelgren B, Kuroyama MC, McBratney-Owen B, Spence AA, Malahn LE, Anawati M, Cabatbat C, Alarcon VB, Marikawa Y, Lozanoff S (2008) Misexpression of *Six2* is associated with heritable frontonasal dysplasia and renal hypoplasia in 3H1 Br mice. Dev Dyn 237:1767–1779. doi:10.1002/dvdy.21587
38. Gendron-Maguire M, Mallo M, Zhang M, Gridley T (1993) *Hoxa2* mutant mice exhibit homeotic transformation of skeletal elements derived from cranial neural crest. Cell 75:1317–1331. doi:10.1016/0092-8674(93)90619-2
39. Rijli F, Mark M, Lakkaraju S, Dierich A, Dolle P, Chambon P (1993) A homeotic transformation is generated in the rostral branchial region of the head by disruption of *Hoxa2*, which acts as a selector gene. Cell 75:1333–1349. doi:10.1016/0092-8674(93)90620-6
40. Kanzler B, Kuschert SJ, Liu YH, Mallo M (1998) *Hoxa-2* restricts the chondrogenic domain and inhibits bone formation during development of the branchial area. Development 125:2587–2597 ISSN: 0950–1991
41. Barrow JR, Capecchi MR (1999) Compensatory defects associated with mutations in *Hoxa1* restore normal palatogenesis to *Hoxa2* mutants. Development 126:5011–5026 ISSN: 0950–1991
42. Bobola N, Carapuco M, Ohnemus S, Kanzler B, Leibbrandt A, Neubuser A, Drouin J, Mallo M (2003) Mesenchymal patterning by *Hoxa2* requires blocking Fgf-dependent activation of Pitx1. Development 130:3403–3414. doi:10.1242/dev.00554
43. Trumpp A, Depew MJ, Rubenstein JL, Bishop JM, Martin GR (1999) Cre-mediated gene inactivation demonstrates that FGF8 is required for cell survival and patterning of the first branchial arch. Gen Dev 13:3136–3148. doi:10.1101/gad.13.23.3136
44. Abu-Issa R, Smyth G, Smoak I, Yamamura K, Meyers EN (2002) Fgf8 is required for pharyngeal arch and cardiovascular development in the mouse. Development 129:4613–4625 ISSN: 0950–1991